A POSSIBLE ORDINARY CHONDRITE AFFINITY FOR METAL FROM THE UNIQUE CHONDRITE NWA 5492. M. Humayun[1] and M. K. Weisberg[2,3], [1]Dept. of Earth, Ocean & Atmospheric Science, and National High Magnetic Field Laboratory, Florida State University, Tallahassee, FL 32310 (humayun@magnet.fsu.edu), [2]Dept. Phys. Sci., Kingsborough Community College and Graduate Center, CUNY, Brooklyn, NY 11235, USA [3]Dept. Earth Planet. Sci., American Museum Natural History, NY, NY 10024 (Michael.Weisberg@kbcc.cuny.edu).

Introduction: NWA 5492 is a new metal-rich chondrite with large (mm-size) metal nodules, lithic clasts and chondrules, lacking visible matrix [1-2]. The high metal/silicate ratio is similar to CB and CH chondrites. Unlike in carbonaceous chondrites, the oxygen isotopes plot above the terrestrial fractionation line between ordinary and enstatite chondrites. Silicates are highly reduced with Fa<1%, Fs<1.5%. The metal composition plots off the chondritic Co vs. Ni trend observed in CR, CH and CB metal to higher Co. The chemical composition shows chondritic Ca/Mg and Al/Mg ratios, with a striking depletion in the Mn/Mg ratio, and Fe/Mg and Ni/Mg ratios that are about 2xCI [2]. A possible relation to the metal-rich unique chondrite GRO 95551 has been proposed [1]. While not a member of any of the three major chondrite classes, NWA 5492 has textural, chemical and oxygen isotopic characteristics that alternatively point to CB-CH, E or O chondrites.

The siderophile element abundances of metal for each of the chondrite groups are distinct. Further, the unique chondrite GRO 95551 was shown to have metal with affinities to ordinary chondrites [3]. To examine the relationship of the metal nodules in NWA 5492 to metal in GRO 95551 and other chondrites, we analyzed siderophile elements by LA-ICP-MS.

Samples and Analytical Methodology: Section NWA 5492-2 (AMNH) from the petrological study of [1] was analyzed using a New Wave UP193FX excimer LA-ICP-MS system at the Plasma Analytical Facility, FSU [4]. Ten metal nodules, >1 mm in size, were selected for analysis. A spot size of 100 µm, with 60 laser shots, and 2 GW/cm^2 was used for most spots, but one analysis was taken with a line scan using 50 µm spot size scanned at 10 µm/s.

Results: Of the ten metal nodules analyzed, one was dominated by a schreibersite grain. The other metals were low in Si, V and Cr. Elemental abundances for the 9 nodules are similar so a single average was calculated and is shown in Fig. 1 on a Ni- and CI-normalized plot. NWA 5492 metal has a CI chondritic Fe/Ni ratio, but exhibits a small positive Co anomaly due to the presence of troilite and schreibersite. Unlike metal from carbonaceous chondrites, NWA 5492 metal has a fractionated refractory siderophile element pattern similar to those from ordinary and enstatite chondrites, with high W and Re, and low Os, Ir, Pt relative to CI.

Discussion: *Relationship to major chondrite groups*: NWA 5492 metal does not show the characteristic enrichments of Au and As observed in EL and EH metal [5], but has a CI chondritic Au/Ni ratio, a feature not shared by CR, CH and CB metal that have sub-chondritic Au/Ni ratios. Fig. 1 shows bulk metal from equilibrated H, L, and LL chondrites [6] compared with metal from NWA 5492. Also shown is the bulk H chondrite composition [7]. The metal from ordinary chondrites form a reduction sequence with the elements W, Fe, Ga, and Mo, depleted relative to H chondrites in the sequence LL metal>L metal> H metal> NWA 5492 metal. Metal from NWA 5492 has siderophile element abundances that are nearly identical to H chondrite bulk composition except that Ni, Pd, Fe and Au are ~10-15% higher than most of the other siderophiles. Metal from NWA 5492 lacks the W, Fe, and Ga depletion seen in metal from H4-6 chondrites because it is more reduced. Anomalies at Mo and Cu are due to partitioning into sulfides.

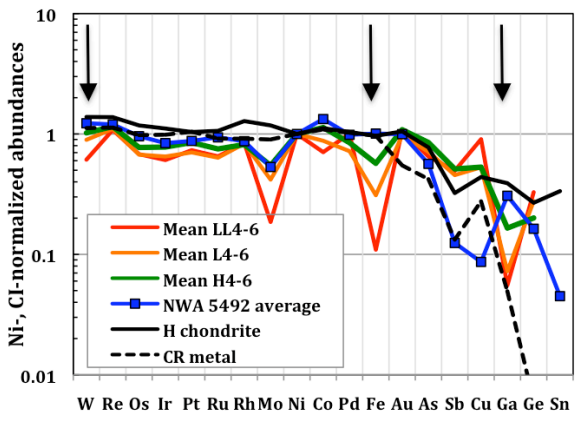

Fig. 1. Siderophile element pattern of NWA 5492 metal compared with metal from equilibrated ordinary chondrites and bulk H chondrite composition [5-8].

To examine the reduction sequence further, the $(W/Ni)_{CI}$ ratio is plotted against the $(Fe/Ni)_{CI}$ ratio in Fig. 2. On this plot, CI chondritic composition plots at unity, CR metal [8] plots close by, while bulk H chondrite plots to high $(W/Ni)_{CI}$ ratio ~1.4xCI, with a chondritic $(Fe/Ni)_{CI}$ ratio. Metal from equilibrated LL, L, H, EL and EH metal plot along a trend of increasing

$(W/Ni)_{CI}$ correlated with $(Fe/Ni)_{CI}$ towards the bulk H chondrite composition. Individual metal grains from NWA 5492 plot on a vertical array with eight of the nine nodules defining a constant $(Fe/Ni)_{CI}$ =1.01±0.02, but exhibiting variable $(W/Ni)_{CI}$ ratios from CI to H chondrite composition. Because W is less siderophile than Fe at T<1200 K [9] metamorphic re-equilibration will cause the $(W/Ni)_{CI}$ ratio to increase. Bulk metal from unequilibrated ordinary chondrites exhibits a $(W/Ni)_{CI}$ ratio that is lower than that of metal from equilibrated ordinary chondrites, and reduction of W from the silicate matrix increases the $(W/Ni)_{CI}$ ratio of metal during equilibration [9].

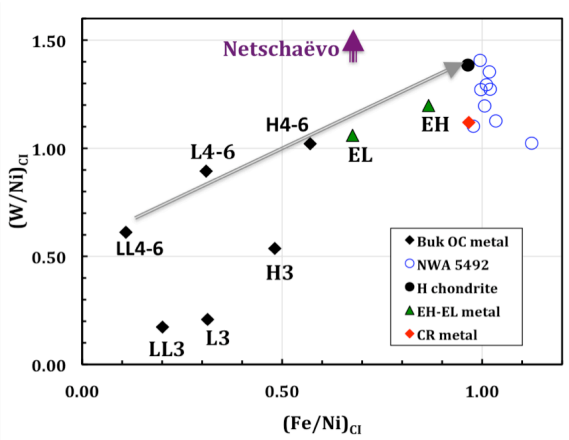

Fig. 2. Reduction sequence in equilibrated ordinary chondrite metal [5], E chondrite metal [6], compared with metal from NWA 5492, and CR chondrites [8]. Netschaëvo metal [11-12] is shown as the purple arrow plotting to $(W/Ni)_{CI}$ ~1.7-2.2.

Relationship to GRO 95551: The unique, metal-rich chondrite GRO 95551 exhibits important similarities to NWA 5492 in texture and oxygen isotope composition [1, 10], except silicates in GRO 95551 include a larger range of Fa compositions [1]. Metal from GRO 95551 exhibits kamacite-taenite exsolution [3], increasing the uncertainty of the bulk GRO 95551 metal composition. The siderophile element pattern of average GRO 95551 metal is shown in Fig. 3, compared with NWA 5492 metal and H chondrite. The two metal-rich chondrites have nearly identical metal composition, similar to the siderophile element pattern of H chondrite. Differences in the absolute siderophile element abundances normalized to Ni are dependent on the kamacite-taenite ratio in GRO 95551. Depletions of Mo and Cu are due to partitioning into troilite, while discrepancies at Sb and Sn are not well understood. For our purpose, the metal from these two chondrites is sufficiently similar in composition to support grouping the two meteorites, based on oxygen isotopes [10].

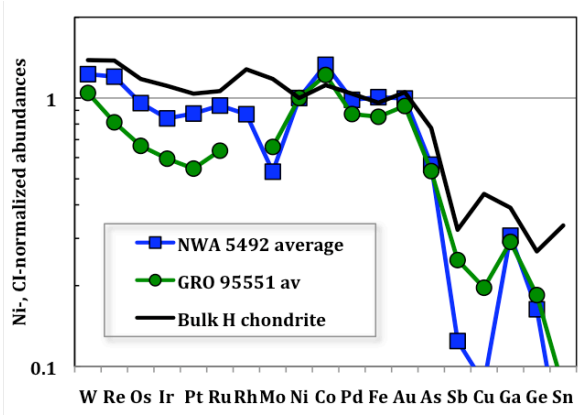

Fig. 3. Comparison of metal from NWA 5492 and GRO 95551 [3] with bulk H chondrite composition [7].

Relationship to HH and low-FeO ordinary chondrites: Ordinary chondrites more reduced than H chondrites but with similar bulk Fe/Si have been described as a low-FeO group [13-14]. A reduced, metal-rich ordinary chondrite group (HH chondrites) was proposed for Netschaëvo [11-12, 15], and linked to the parental material of IIE irons [11-12]. NWA 5492 is a unique chondrite, linked to GRO 95551 [1], which is both more metal-rich and more reduced than H chondrites but with a similar siderophile element pattern. However, silicates in NWA 5492 (Fa<1% [1]) are much more reduced than silicates in low-FeO OCs (Fa 13-16, [13-14]), Netschaëvo (Fa 14 [16]), or silicates from IIE irons (Fa 14-17 [12]). This is also seen in the Ni content of the metal: NWA 5492 (4.9-5.4%) vs. Netschaëvo (8.6% [11]), IIEs (7.2-9.7% [11-12]) and H4-6 metal (8-10% [5]). We conclude that NWA 5492 is too reduced to be the parental material of IIEs or to be grouped with Netschaëvo as a member of a new HH chondrite group. The nature of the reductant for NWA 5492/GRO 95551 and its relationship to the H chondrite parent body is not known, yet.

References: [1] Weisberg M. K. et al. (2012) *MAPS*, submitted. [2] Friend P. et al. (2011) *LPS*, *42*, abstract #1095. [3] Campbell A. J. and Humayun M. (2003) *GCA*, *67*, 2481-2495. [4] Humayun M. et al. (2007) *GCA, 71*, 4609-4627. [5] Kong P. et al. (1997) *GCA*, *61*, 4895-4914. [6] Kong P. and Ebihara M. (1997) *GCA*, *61*, 2317. [7] Teplyakova S. N. et al. (2012) *LPS*, *43*, abstract #1130. [8] Kong P. et al. (1999) *GCA*, *63*, 2637-2652. [9] Humayun M. and Campbell A. J. (2002) *EPSL*, *198*, 225-243. [10] Weisberg M. K. et al. (2012), *LPS*, *43*, this volume. [11] Wasson J. T. and Wang J. (1986) *GCA, 50*, 725-732. [12] Wasson T. and Scott (2011) *LPS, 42,* Abstract #2813. [13] Russell S. S. et al. (1998) *MAPS*, *33*, 853-856. [14] Trioano J. et al. (2011) *GCA*, *75*, 6511-6519. [15] Bild R. W. and Wasson J. T. (1977) *Science*, *197*, 58. [16] Bunch T. E. et al. (1970) *Contrib. Mineral. Petrol.*, *25*, 297-340.